



PCCP

Enhanced performance of dye-sensitized solar cells with dual-function coadsorbent: reducing the surface concentration of dye– iodine complexes concomitant with attenuated charge recombination

Journal:	<i>Physical Chemistry Chemical Physics</i>
Manuscript ID:	CP-ART-06-2015-003428.R2
Article Type:	Paper
Date Submitted by the Author:	23-Jul-2015
Complete List of Authors:	mazloum, mohammad; Yazd University, Department of Chemistry Khoshro, A.; Yazd Uni.,

SCHOLARONE™
Manuscripts

Physical Chemistry Chemical Physics

**Enhanced performance of dye-sensitized solar cells with dual-function
coadsorbent: reducing the surface concentration of dye– iodine
complexes concomitant with attenuated charge recombination**

Mohammad Mazloun-Ardakani*, Alireza Khoshroo

*Department of Chemistry, Faculty of Science, Yazd University, Yazd, 89195-741, I.R. Iran
Iran*

E-Mail: mazloun@yazd.ac.ir

Phone No: 00983518211670

Fax No: 00983518210644

Abstract

In this paper, we have investigated the effects of oleic acid as a dual-function coadsorbent on recombination and iodine binding in dye-sensitized solar cells. Oleic acid as a dual-function coadsorbent effectively shields the back electron transfer from the TiO_2 to I_3^- ions and also reduces the surface concentration of dye- I_2 complexes via iodine binds to the unsaturated double bond on oleic acid. It was found that interaction between iodine and double bond of oleic keep the iodine molecules away from surface and reduce the recombination rate between injected electrons in semiconductor and iodine molecules and increase open-circuit voltage. Furthermore, the interaction between iodine molecules and unexcited dyes affects the UV-vis spectrum of them and prevent to unfavorable blue shift. Overall, the results point to an improved performance for DSC operation and development.

Keywords: dye-sensitized solar cells, oleic acid, recombination, passivation, dye- iodine complex

Introduction

Dye-sensitized solar cells (DSCs) are attracting a wide-spread academic and industrial interest as potential low-cost alternatives to conventional photovoltaic systems¹⁻⁴. A typical cell structure consists of a dye-sensitized nanocrystalline titanium dioxide (TiO₂) film deposited on a transparent conducting oxide (TCO) glass, a platinum counter electrode, and an electrolyte containing a redox couple^{5,6}. In these devices, the surfaces of the TiO₂ are not fully covered by the dye molecules. Therefore, electrons injected into the nanocrystalline TiO₂ layer tend to recombine with either the oxidized form of the dye or the oxidized form of the redox couple, resulting in the loss of efficiency^{7,8}. This electron transfer can occur both at the interface between the TiO₂-electrolyte interface and at the part of the TCO that is exposed to the electrolyte⁹. In particular, the electron recombination with iodine (rather than tri-iodide) at the TiO₂-electrolyte interface is known to be quite important in deteriorating the photovoltaic performance¹⁰. This electron recombination could be reduced or eliminated by selectively coating an insulating and transparent layer on these open area of TiO₂. For minimizing such losses in DSCs various approaches have been used, such as coating of inorganic barrier layers¹¹⁻¹⁴ and the introduction of coadsorbents¹⁵⁻¹⁸.

The formation of complexes between iodine and organic molecules has long been recognized as an important phenomenon¹⁹⁻²¹. Näther et al.²² indicate that iodine binds to sulfur atom through its lone pair electron. A major challenge for N719 molecules as sensitizers in DSCs is the iodine binding that occurs between the sulphur and/or nitrogen atoms of dyes and iodine, which presents unfavorable effects on the DSC performance^{23,10}. These spectrum shifts can be related to the change of dyes orbitals' energy levels

and the V_{oc} loss in cells. Recently, the interaction between iodine–dye, and its effect on recombination has been described¹⁰. O'Regan et al. have indicated that the interaction between iodine and dyes adsorbed on TiO_2 surface in dye-sensitized solar cells influence on cell performance^{24–26}. The binding of iodine to ruthenium dyes²⁵, has been suggested to increase recombination of conduction band electrons to the electrolyte. The increase in recombination from dye–iodine binding could result from an increase the local iodine concentration near the TiO_2 surface^{27,28}. O'Regan et al.²⁶ presented a strategy for decreases of dye–iodine binding based on p-aminobenzoic acid on the TiO_2 surface. The recombination can be decreases by adsorption of p-aminobenzoic acid on the TiO_2 surface, likely due to iodine binding to the amine group.

In this work, we report the findings a new dual-function coadsorbent of molecular insulators that electronically passive the surface of nanocrystalline TiO_2 films. Oleic acid as a coadsorbent containing hydrophobic alkyl chain is serving as buffers blocking water and triiodide from the surface of TiO_2 . Furthermore, we find the evidence for interaction between iodine and oleic acid via the double bond of oleic. Adsorption of oleic acid on the TiO_2 surface decreases the recombination due to iodine binding to the double bond of oleic acid. Then, it may be concluded that, the adsorption of oleic acid on the TiO_2 surface decreases the recombination due to iodine binding to the double bond of oleic acid, and enhances the performance of DSC.

2. Experimental

2.1. Apparatus and chemicals

All of the materials used in this work were used as received, without further purification, if not stated otherwise. The N719 dye and FTO glasses were purchased from Dyesol. 4-tert-butylpyridine, guanidinium thiocyanate, H_2PtCl_6 and 1-butyl-3-methylimidazolium (BMII) were reagent-grade from Sigma Aldrich. Iodine, valeronitrile, solvents and reagents were of pro-analysis grade from Merck (Darmstadt, Germany). TiCl_4 (Merck) was diluted with water to 2.0 M at 0 °C to make a stock solution, which was kept in a freezer and freshly diluted to 40.0 mM with water for each TiCl_4 treatment of the FTO coated glass plates.

The active surface area of films was determined by dye-loading in 4 mL of NaOH (0.1 M in DI water) and estimating the concentration of dye using absorption measurements (Optizen 3220 UV–Vis spectrophotometer). The DSC performance was evaluated in AM 1.5 simulated light (Luzchem-Solar) using a potentiostat/galvanostat (IVIUM, Compactstat). The absorption spectra of the N719/ TiO_2 film were recorded using a UV-vis spectrophotometer. We investigated the dye-iodine-oleic acid interaction by measuring the absorption spectra of N719/ TiO_2 films during iodine and oleic acid addition in acetonitrile. Iodine and oleic acid titration was carried out in a 1.0 cm cell containing 2 mL acetonitrile. The N719/ TiO_2 films on 0.1 cm FTO were placed on one side of the cell. This allowed the measurement of the spectrum of the film and solution, and, by rotation of the cell (90 degrees), the measurement of the spectrum of the solution alone. The absorbance of the N719/ TiO_2 films alone (OD_{film}) was obtained by subtraction of the solution spectrum from that of the film plus solution by use of this equation, $\text{OD}_{\text{film}} = \text{OD}_1 - 0.9 \times \text{OD}_2$, where OD_1 is the absorbance of N719/ TiO_2 films in iodine-

oleic acid solution and OD2 is the absorbance of iodine- oleic acid; the factor 0.9 corrects the beam pathway (10 mm) by subtracting the thickness of the microscope slide (1 mm).

2.2. Solar Cells Fabrication

FTO glass was used for transparent conducting electrodes. The substrate was first cleaned in an ultrasonic bath using a detergent solution, acetone, and ethanol, respectively (each step was 15 min long). The FTO glass plates were immersed into a 40 mM aqueous TiCl_4 solution at 70°C for 30 min and washed with water and ethanol.

The screen-printable 20 nm TiO_2 paste was prepared according to the procedures described in the literature⁵. A layer of TiO_2 paste was spread on the FTO glass plates by doctor blade. The samples were finally sintered at 500 °C for 30 min. After the sintering process, the TiO_2 film was treated with 40 mM TiCl_4 solution, then rinsed with water and ethanol. The electrodes were heated at 500°C for 30 min. After cooling to 80 °C, the TiO_2 electrode was immersed into a 0.3 mM N719 dye solution in a mixture of acetonitrile and tertbutyl alcohol (volume ratio, 1:1) or sensitized with N719 and oleic acid (denoted to electrode A and B, respectively) and kept at room temperature for 20 h to assure complete sensitizer uptake.

The counter electrode was prepared on a perforated FTO-glass according to previously reported methods⁵. The working and counter electrodes were assembled into a sandwich cell, and sealed with a hot-melt gasket of 35- μm thickness made of surlyn (Dyesol), they filled with the redox-active electrolyte throughout the present study consisted of 0.6 M 1-butyl-3-methyl imidazolium iodide (BMII), 0.03 M I_2 , 0.10 M

guanidinium thiocyanate and 0.5 M 4-tertbutylpyridine in a mixture of acetonitrile and valeronitrile (volume ratio, 85:15)²⁹.

3. Results and discussion

3.1. Dye and Coadsorbent Adsorption Behavior

UV-vis measurements were performed to analyze the adsorption amount of dye N719 in the TiO₂ electrodes (Fig. 1). N719 was desorbed from the TiO₂ film by immersing the sensitized electrodes into 0.1 M KOH aqueous solutions. Oleic acid at concentration of 0.3 mM yielded absorption intensities of 71%; this value dramatically decreased as the concentration of coadsorbent was increased by a factor of 10 (to 3.0 mM). The absorption intensity reached 14% at a concentration 10 times higher (3.0 mM). The relative adsorption intensities of dye loaded in the TiO₂ film was 71% for electrode-B as compared to the electrode A for optimal concentration. This decrease was in good agreement with previous work^{30,31}. The coadsorbent retards the rate of dye adsorption via a competitive anchoring process, thereby increasing the surface concentration of strongly bound dye and decreasing the dye aggregation on the TiO₂ surface³². Therefore, the decrease of dye loading in this study suggested that the competitive equilibrium anchoring process may disfavor the formation of dye aggregates on the surfaces of the nanocrystalline TiO₂ electrode³⁰.

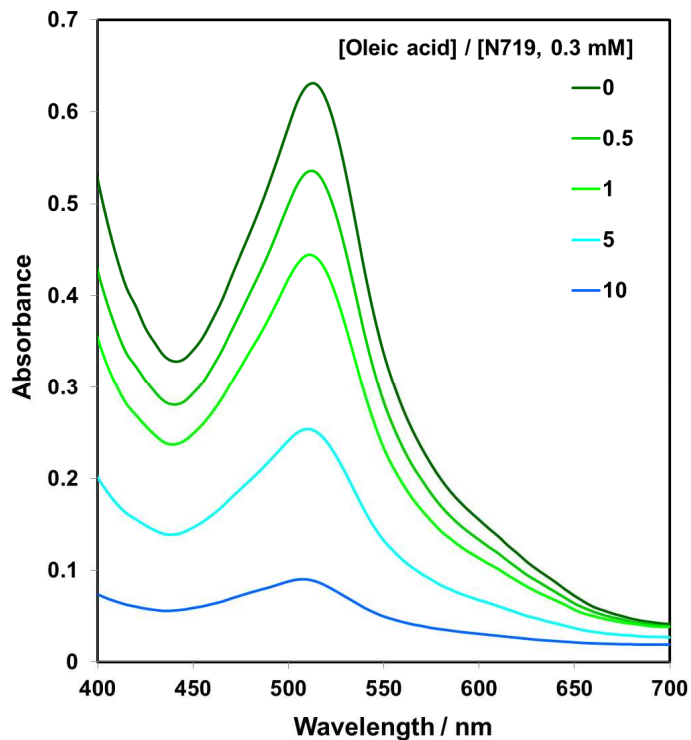


Fig. 1 The UV-Vis spectra of the dye (N719) and either oleic acid detached from the TiO₂ electrodes removed by immersion in a 0.1 M KOH aqueous solution.

3.2. Photovoltaic Characterization

The photovoltaic performances of the devices were measured under AM 1.5 solar conditions to measure the effect of the different molar ratio of oleic acid on J_{SC} and V_{OC} (Table 1). Fig. 2 shows the photocurrent–voltage curves of the DSCs sensitized with N719 dye alone (device A) and with oleic acid (device B [oleic acid]) as the coadsorbent measured under AM 1.5 full sunlight. In device A, TiO₂ electrode stained with the N719 sensitizer alone give rise to photovoltaic conversion efficiency (η) of 6.45 % (J_{sc} =14.02 mA cm⁻², V_{OC} =754 mV, and FF=61.2%), as shown in Entries 1. While N719 is combined with oleic acid as the sensitizer in a molar ratio from 2 to 0.1 (Entries 2–4),

the η increase to 6.94% ($J_{sc}=14.58 \text{ mA cm}^{-2}$, $V_{OC}=762 \text{ mV}$, and $FF=62.5\%$) at the half molar ratio of oleic acid (Entry 2) then increases to the highest point of 7.65% (Entry 3) at the equivalent molar ratio of oleic acid to N719. Further increase in oleic acid content causes efficiency falling down (Entry 4-5). By comparing the corresponding device performances, the optimum concentration of oleic acid as the coadsorbent for sensitization was selected as 0.3 mM.

It is noteworthy that device-B [0.3] yielded an 9.8% and 4.5% improvement in J_{sc} and V_{OC} , respectively, at a 29% lower N719 coverage, to yield a 18.5% improvement in efficiency. The oleic acid affects mainly on the photocurrent, but the η improvement is attributed to the enhanced V_{OC} coupled with the photocurrent. In the following section, for comparison, we will only discuss the devices modified by the oleic acid at the optimal concentration (0.3 mM).

Dark current, resulting from the reduction of tri-iodide by the conduction band electrons of TiO_2 , was crucial to the properties of the cells in respect that it revealed the situation of surface state and energy level of TiO_2 . The dark current data in insert Fig. 2 suggest that the mixed monolayer of N719 and oleic acid is more effective in retarding this back reaction, a finding consistent with the $\sim 30 \text{ mV}$ increase in V_{OC} . Therefore, adsorption of dye with oleic acid as a coadsorbent reduces the charge recombination, which detailed analysis is given later via electrochemical analysis.

Table 1 Photocurrent–voltage characteristics ^a for DSCs sensitized with N719 (electrode A) or N719 plus oleic acid (electrode B).

Entry	Relative [dye] ^b	V _{oc} /mV	J _{sc} /mA cm ²	FF (%)	η (%)
electrode A	1.00	754	14.02	61.2	6.45
electrode B (0.15)	0.84	762	14.58	62.5	6.94
electrode B (0.3)	0.71	786	15.39	63.2	7.65
electrode B (1.5)	0.41	759	13.52	60.3	6.20
electrode B (3.0)	0.14	739	11.81	57.6	5.03

^aValues obtained using the average over 6 devices for each experiment.

^bDetermined by measuring UV-Vis absorption spectra.

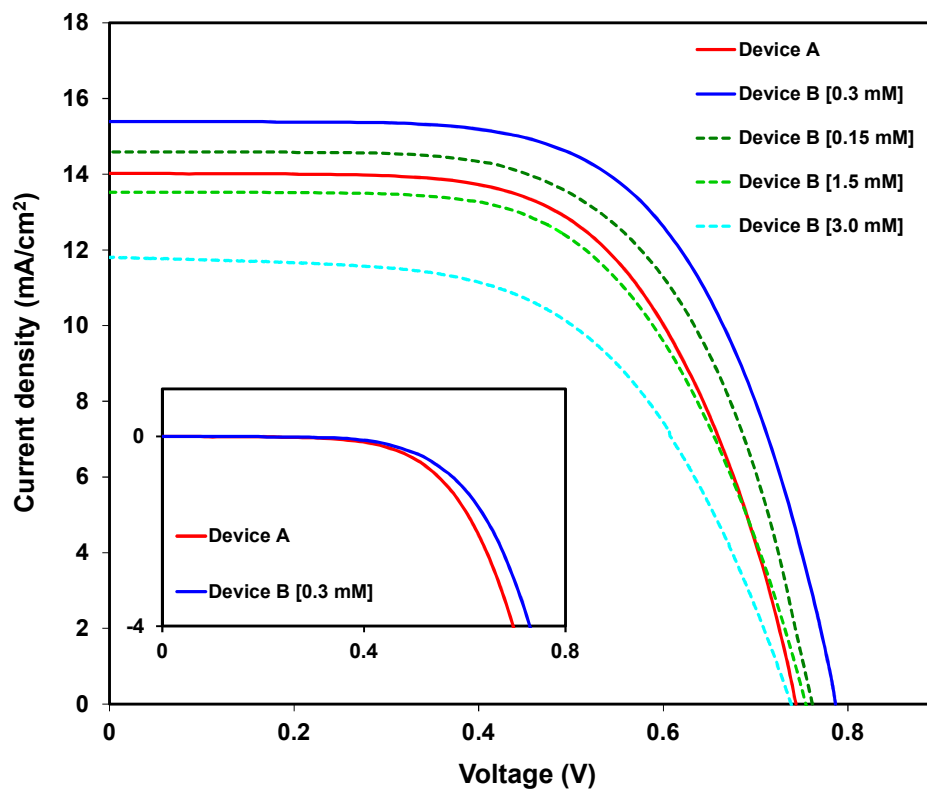


Fig. 2 The photocurrent–voltage curves of the device sensitized with N719 dye alone (device A) and with oleic acid (device B [oleic acid]) under AM 1.5 simulated sunlight illumination, Inset: In the dark condition

3.3. The analysis of J_{SC}

O'Regan et al.¹⁰ reported that the direct evidence for dye–iodine binding to dye via the thiocyanate group of the N719 dye. They showed when iodine binds to the NCS^- ligands, the energy of the HOMO decreases, blue shifting any HOMO→LUMO transitions, including the visible and UV MLCT bands. Then to find out the effect of this in our case we have studied the interaction between iodine molecules with N719 and oleic acids.

The absorption spectra of N719/TiO₂ film in mixture of acetonitrile and tertbutyl alcohol (volume ratio, 1:1) solution alone or with iodine and oleic acid are shown in Fig. 3. In this Fig, we observe a 45 nm blue shift in intensity from the MLCT peak at 535 nm to a new peak about 490 nm. A blue shift in absorbance can be caused by a decrease in the HOMO energy, and/or an increase in the LUMO energy¹⁰. When oleic acid added in solution, a red shift in peak was observed from 490 nm to 529 nm. We suggest this may be because the iodine bound to the unsaturated double bond on oleic acid. Thus the reactivity of the bound iodine will be less than the free iodine at the same distance from the surface, by an amount related to the specifics of binding. Based on this result, adsorption of oleic acid on the TiO₂ surface caused red shifts the peak, likely due to iodine binding to the unsaturated double bond on oleic acid. Therefore, the interactions between iodine and double bond of oleic keep the iodine molecules away from thiocyanate group of dyes affects the UV-vis spectrum of them and prevent to unfavorable blue shift.

Another reason for the increase enhancement of photocurrent due to the competition of the oleic acid with dye N719 for the limited sites of TiO₂ surface in the co-adsorption process¹⁸. The competitive adsorption retards the rate of dye adsorption, reduces the weakly bonded dye and prevents the aggregation of dye molecules on the TiO₂ surface, which minimizes the intermolecular energy transfer, increases the electron injection efficiency and leads to the enhancement of J_{SC}. Oleic acid may induce change in the adsorption state of dye and electronic state of dye-sensitized TiO₂, thereby the electron injection rate and efficiency could be influenced^{18,16}. Therefore, a part of the improved J_{SC} for device B compared with device A may be ascribed to the breakup of

dye aggregates because of the competitive adsorption of N719 with the oleic acid. The decrease in J_{sc} at a high concentration of oleic acid (oleic acid to dye ratios greater than 1:1) would result from the insufficient dye regeneration rate because of the shielding of the approach of iodides to oxidized dye molecules by the excessive occupation of long coadsorbent chains on the TiO_2 interfaces.

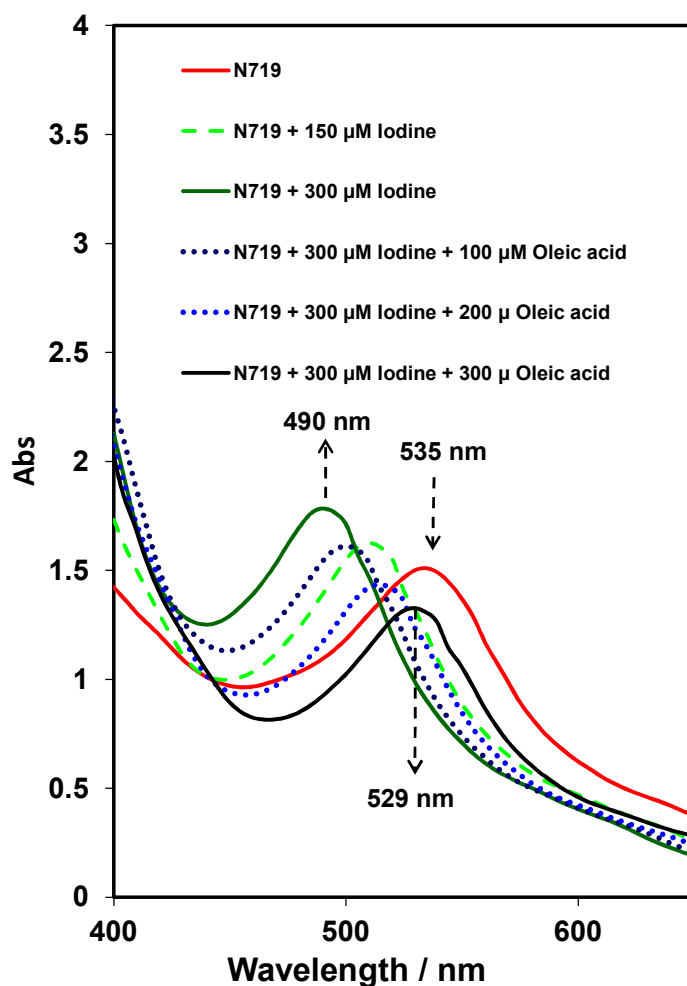


Fig. 3 The absorption spectra of N719/ TiO_2 film in mixture of acetonitrile and tertbutyl alcohol (volume ratio, 1:1) solution alone or with iodine and oleic acid. Iodine and oleic acid concentrations as listed in the legends.

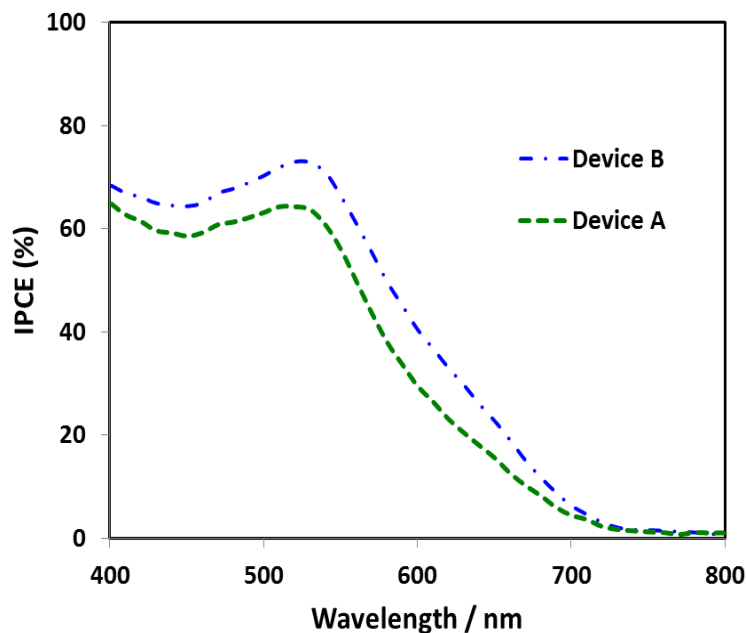


Fig. 4 The IPCE curves of the device sensitized with N719 dye alone (device A) and with oleic acid (device B)

The measurement of the incident photon-to-current conversion efficiency (IPCE) as a function of wavelength was carried out in order to gain an insight to the increased J_{SC} in the presence of oleic acid. As shown in figure 4, the increased IPCE performance was observed from the devices with oleic acid co-adsorbent.

The increased quantum yield is ascribed to the inhibited dye aggregation in the presence of oleic acid as co-adsorbent, which minimizes the intermolecular energy transfer and increases the electron injection efficiency³³. As a result, it compensates the loss of light harvesting caused by lower dye coverage in the TiO_2 photoanode with oleic acid as the co-adsorbent and leads to the enhancement of J_{SC} ³⁴.

3.4. The analysis of V_{OC}

The V_{OC} value of DSCs is related to the quasi Fermi level ($E_{F,n}$) and the redox potential (E_{redox}) of electrolyte. Supposing E_{redox} as a constant, V_{OC} will be controlled by the $E_{F,n}$ of TiO_2 . The $E_{F,n}$ can be described as follows ³⁵:

$$E_{F,n} = E_{CB} + k_B T \ln(n / N_{CB}) \quad (1)$$

Here, E_{CB} is the conduction band edge of TiO_2 , T is the absolute temperature, k_B is the Boltzmann constant, N_{CB} is the effective density of states and n is the number of electrons in TiO_2 related to the carrier transfer processes including the electron injection and recombination. Based on the equation (1), $E_{F,n}$ can be elevated either by the movement of the E_{CB} to vacuum level or by the increased electron population in TiO_2 , eventually causing an enhancement in V_{OC} ³⁶. In order to further understand the mechanisms of the increase of V_{OC} in our case, cyclic voltammetry and EIS were performed for changes in E_{CB} and concentration of electrons in the film.

In order to investigate the change in the trap state induced by the oleic acid and to reveal the change in V_{OC} , cyclic voltammetry was performed on TiO_2 electrode stained with the N719 sensitizer alone (curve a, Fig. 5a) or in combination with oleic acid (curve b, Fig. 5a). The capacitive currents in the forward scan as shown in Fig. 5b of the electrodes displayed gradual onsets. As shown in this Fig., the onset was around -0.79 V for the TiO_2 electrode stained with the N719 sensitizer alone (Electrode A) having a direct contact with the electrolyte, whereas the electrode A covered with oleic acid displayed onsets in the -0.81 V. This observation indicates that the edge of conduction band of TiO_2 slightly has changed ³⁰. Moreover, the slope (dQ/dV , where Q is the total number of surface trapping sites and V is the potential applied to the electrode) of

electrode A was large, and the slope decreased after combination with oleic acid (electrode-B). This indicated that the reduction in the number of surface trapping sites at which photoinduced electrons could recombine with oxidized species¹⁶.

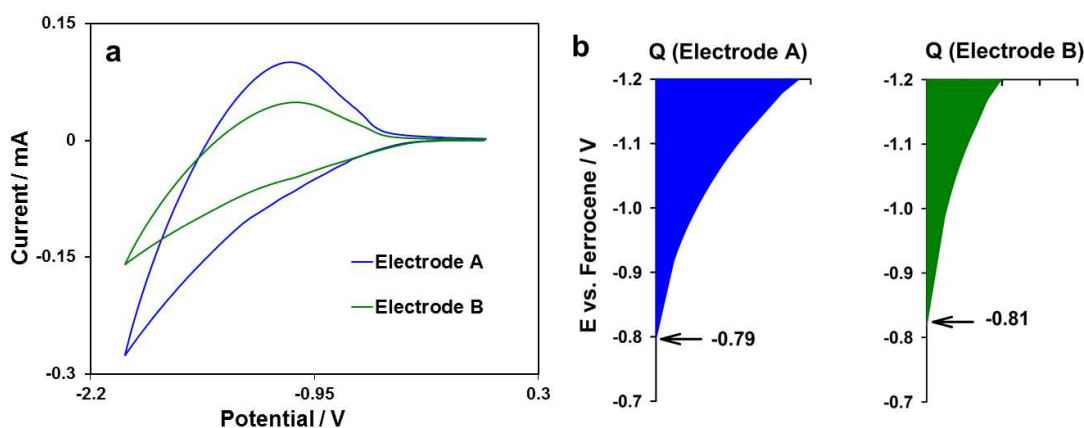


Fig. 5 (a) CVs of electrode A (N719 dye) and electrode B (N719 dye with oleic acid) in BMIB, The scan rate is 0.05 Vs^{-1} . (b) Energy levels at the TiO_2/BMIB interface.

In order to investigate the influence of oleic acid on the electron population in TiO_2 , EIS was performed on each TiO_2 electrode sensitized with N719 alone (device A) and with oleic acid (device B) in the dark. In Figure 6, the Nyquist plots consist of two semicircles. The smaller semicircle occurring at higher frequencies represents the charge-transfer resistance at the counter electrode/electrolyte interface, while the larger one at lower frequencies is attributed to the resistance at the $\text{TiO}_2/\text{electrolyte}$ interface. R_{ct} was estimated to be 71Ω for the cells treated with N719 alone and 132Ω for those with N719 to oleic acid ratio of 1:1. The smaller R_{ct} value means that the electron recombination from the conduction band to the electrolyte occurs more easily, thus resulting in lower V_{oc} . Clearly, the electron recombination in devices based on N719 alone is faster than

that of N719 and oleic acid. This result clearly states that oleic acid as the coadsorbent exhibits strong ability to suppress the back electron transfer. Electron lifetime (τ), as another significant parameter to evaluate the charge recombination rate, is usually obtained by R_{rec} and $C\mu$ ($\tau = R_{\text{ct}} * C\mu$) from EIS by fitting the experimental data through an appropriate equivalent circuit³⁷. By comparing device A with device B, τ increased from 30.6 ms to 68.5 ms. This result clearly states that oleic acid as the coadsorbent exhibits strong ability to suppress the back electron transfer.

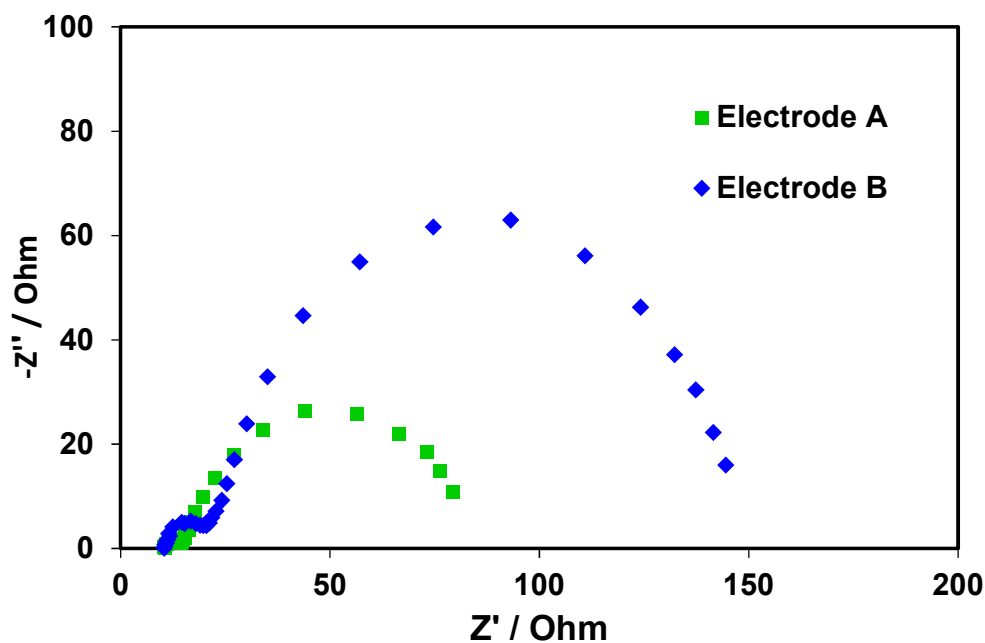


Fig. 6 The electrochemical impedance spectra of the device sensitized with N719 dye alone (device A) and with oleic acid (device B) under the dark condition.

This property can be attributed to that (1) the large alkyl chain of yields longer distance between the electrons in the TiO_2 and I^{3-} in the iodide electrolyte; (2) interaction between iodine and double bond of oleic keep the iodine molecules away from surface,

which could reduce the recombination rate between injected electrons in semiconductor and iodine molecules. Therefore, the increased V_{OC} of the device B is due to the increasing of the electron population in TiO_2 and the shift of the conduction band of TiO_2 . A further increase in the oleic acid-to-dye ratio to 1:1 (Entry 2 in Table 1) leads to a decrease in V_{oc} . This phenomenon is due to the extra protons formed at surface from $-COOH$ to TiO_2 surface forming interfacial dipoles results in a shift in the band-edge at the interface, which explains the decrease in the V_{oc} ^{38,39}.

4. Conclusions

It was found that the introduction of the oleic acid as a dual-function coadsorbent in DSC afforded the device with higher V_{OC} , J_{SC} and photovoltaic conversion efficiency. We contribute such performance to the structure of oleic acid and the iodine-bonding interaction of unsaturated double bond on oleic acid, which widens the spatial separation between the TiO_2 surface and the acceptors in the electrolyte. Furthermore, the interaction between iodine molecules and dyes affects the UV-vis spectrum of them and prevents an unfavorable blue shift. Moreover, the competitive anchoring process of oleic acid and N719 on the TiO_2 surface effectively diminishes the aggregation of dye molecules, which minimizes the intermolecular energy transfer, increases the electron injection efficiency and leads to the enhancement of photovoltaic conversion efficiency. Finally, we demonstrated that the resulting DSC devices satisfied two criteria: (1) reduced dye loading, (2) simultaneous improvements in J_{SC} and V_{OC} .

Acknowledgements

The authors wish to thank the Yazd University Research Council, IUT Research Council and Excellence in Sensors and Yazd Regional Electric Company for financial support of this research.

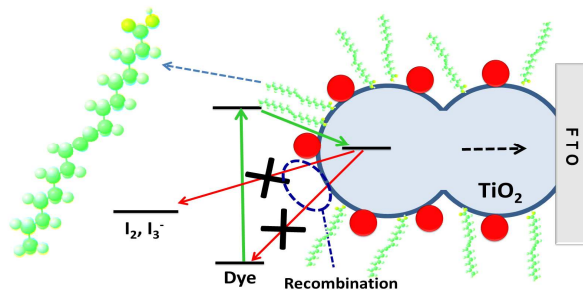
References

1. B. O'regan and M. Grätzel, *Nature*, 1991, **353**, 737–740.
2. A. Hagfeldt, G. Boschloo, L. Sun, L. Kloo, and H. Pettersson, *Chem. Rev.*, 2010, **110**, 6595–6663.
3. T. M. Brown, F. De Rossi, F. Di Giacomo, G. Mincuzzi, V. Zardetto, A. Reale, and A. Di Carlo, *J. Mater. Chem. A*, 2014, **2**, 10788–10817.
4. B. O'Regan, F. Lenzmann, R. Muis, and J. Wienke, *Chem. Mater.*, 2002, **14**, 5023–5029.
5. S. Ito, T. N. Murakami, P. Comte, P. Liska, C. Grätzel, M. K. Nazeeruddin, and M. Grätzel, *Thin Solid Films*, 2008, **516**, 4613–4619.
6. P. M. Sommeling, B. C. O'regan, R. R. Haswell, H. J. P. Smit, N. J. Bakker, J. J. T. Smits, J. M. Kroon, and J. A. M. Van Roosmalen, *J. Phys. Chem. B*, 2006, **110**, 19191–19197.
7. S. E. Koops, P. R. F. Barnes, B. C. O'Regan, and J. R. Durrant, *J. Phys. Chem. C*, 2010, **114**, 8054–8061.
8. A. Listorti, B. O'Regan, and J. R. Durrant, *Chem. Mater.*, 2011, **23**, 3381–3399.
9. B. C. O'Regan and J. R. Durrant, *Acc. Chem. Res.*, 2009, **42**, 1799–1808.
10. X. Li, A. Reynal, P. Barnes, R. Humphry-Baker, S. M. Zakeeruddin, F. De Angelis, and B. C. O'Regan, *Phys. Chem. Chem. Phys.*, 2012, **14**, 15421–15428.
11. H.-J. Son, X. Wang, C. Prasittichai, N. C. Jeong, T. Aaltonen, R. G. Gordon, and J. T. Hupp, *J. Am. Chem. Soc.*, 2012, **134**, 9537–9540.
12. T. C. Li, M. S. Góes, F. Fabregat-Santiago, J. Bisquert, P. R. Bueno, C. Prasittichai, J. T. Hupp, and T. J. Marks, *J. Phys. Chem. C*, 2009, **113**, 18385–18390.
13. J. Idígoras, G. Burdziński, J. Karolczak, J. Kubicki, G. Oskam, J. A. Anta, and M. Ziółek, *J. Phys. Chem. C*, 2015, **119**, 3931–3944.
14. B. C. O'regan, S. Scully, A. C. Mayer, E. Palomares, and J. Durrant, *J. Phys. Chem. B*, 2005, **109**, 4616–4623.
15. J. Xu, H. Wu, X. Jia, H. Kafafy, and D. Zou, *J. Mater. Chem. A*, 2013, **1**, 14524–14531.

16. Z. Zhang, S. M. Zakeeruddin, B. C. O'Regan, R. Humphry-Baker, and M. Grätzel, *J. Phys. Chem. B*, 2005, **109**, 21818–21824.
17. L. Han, A. Islam, H. Chen, C. Malapaka, B. Chiranjeevi, S. Zhang, X. Yang, and M. Yanagida, *Energy Environ. Sci.*, 2012, **5**, 6057–6060.
18. N. R. Neale, N. Kopidakis, J. van de Lagemaat, M. Grätzel, and A. J. Frank, *J. Phys. Chem. B*, 2005, **109**, 23183–23189.
19. C. N. R. Rao, S. N. Bhat, and P. C. Dwedi, *Appl. Spectrosc. Rev.*, 1972, **5**, 1–170.
20. H. A. Benesi and J. H. Hildebrand, *J. Am. Chem. Soc.*, 1949, **71**, 2703–2707.
21. H. Liu, J. A. Pojman, Y. Zhao, C. Pan, J. Zheng, L. Yuan, A. K. Horvath, and Q. Gao, *Phys. Chem. Chem. Phys.*, 2012, **14**, 131–137.
22. C. Näther and M. Bolte, *Phosphorus. Sulfur. Silicon Relat. Elem.*, 2003, **178**, 453–464.
23. H. Kusama and K. Sayama, *Phys. Chem. Chem. Phys.*, 2015, **17**, 4379–4387.
24. B. C. O'Regan, I. López-Duarte, M. V. Martínez-Díaz, A. Forneli, J. Albero, A. Morandeira, E. Palomares, T. Torres, and J. R. Durrant, *J. Am. Chem. Soc.*, 2008, **130**, 2906–2907.
25. B. C. O'Regan, K. Walley, M. Juozapavicius, A. Anderson, F. Matar, T. Ghaddar, S. M. Zakeeruddin, C. Klein, and J. R. Durrant, *J. Am. Chem. Soc.*, 2009, **131**, 3541–3548.
26. B. C. O'Regan and J. R. Durrant, *Acc. Chem. Res.*, 2009, **42**, 1799–1808.
27. X. A. Jeanbourquin, X. Li, C. Law, P. R. F. Barnes, R. Humphry-Baker, P. Lund, M. I. Asghar, and B. C. O'Regan, *J. Am. Chem. Soc.*, 2014, **136**, 7286–7294.
28. Z. Sun, M. Liang, and J. Chen, *Acc. Chem. Res.*, 2015.
29. L. Giribabu, T. Bessho, M. Srinivasu, C. Vijaykumar, Y. Soujanya, V. G. Reddy, P. Y. Reddy, J.-H. Yum, M. Grätzel, and M. K. Nazeeruddin, *Dalt. Trans.*, 2011, **40**, 4497–4504.
30. J. Lim, Y. S. Kwon, and T. Park, *Chem. Commun.*, 2011, **47**, 4147–4149.
31. S. Park, J. Lim, I. Y. Song, N. Atmakuri, S. Song, Y. S. Kwon, J. M. Choi, and T. Park, *Adv. Energy Mater.*, 2012, **2**, 219–224.

32. J. Lim, Y. S. Kwon, S.-H. Park, I. Y. Song, J. Choi, and T. Park, *Langmuir*, 2011, **27**, 14647–14653.
33. K. Hara, Y. Dan-oh, C. Kasada, Y. Ohga, A. Shinpo, S. Suga, K. Sayama, and H. Arakawa, *Langmuir*, 2004, **20**, 4205–4210.
34. P. Wang, S. M. Zakeeruddin, R. Humphry Baker, J. E. Moser, and M. Grätzel, *Adv. Mater.*, 2003, **15**, 2101–2104.
35. S. Y. Huang, G. Schlichthörl, A. J. Nozik, M. Grätzel, and A. J. Frank, *J. Phys. Chem. B*, 1997, **101**, 2576–2582.
36. N. Kopidakis, N. R. Neale, and A. J. Frank, *J. Phys. Chem. B*, 2006, **110**, 12485–12489.
37. A. Kay and M. Graetzel, *J. Phys. Chem.*, 1993, **97**, 6272–6277.
38. Y. Liu, S. R. Scully, M. D. McGehee, J. Liu, C. K. Luscombe, J. M. J. Frechet, S. E. Shaheen, and D. S. Ginley, *J. Phys. Chem. B*, 2006, **110**, 3257–3261.
39. W. Yang, M. Pazoki, A. I. K. Eriksson, Y. Hao, and G. Boschloo, *Phys. Chem. Chem. Phys.*, 2015, **17**, 16744–16751.

Graphical abstract



Highlight:

We introduce a dual-function coadsorbent in DSCs, that play a beneficial role in the recombination and iodine binds to the N719 dye.